Journal of Advanced College of Engineering and Management

Performance of Armoured Steel Plate against High-Speed Projectile using Finite Element Analysis and Lab Experiment

[1]Sunil Pathak, [1*]Raj Kumar Chaulagain
[1]*Department of Automobile and Mechanical Engineering, Thapathali Campus, IOE, T.U.*
Corresponding email: [*]rajkrc12@tcioe.edu.np

DOI: 10.3126/jacem.v12i01.93958

Abstract
A comprehensive understanding of the mechanical behavior of armored plates used in defense sectors under high-velocity impact is fundamental in optimizing material selection and design for specific operational requirements. This research investigates the ballistic performance of armoured steel plate through integrated finite element analysis and experimental testing. The study began with the mechanical property characterization of the armoured steel plate, from which Johnson-Cook (JC) constitutive parameters were derived by correlating with established literature. Using a finite element analysis explicit dynamic solver for the simulation of multiple impact scenarios, with simulation predictions validated against experimental test data. The experimental data of high-velocity impact from a leaded projectile at 30^0, 60^0, and 90^0 incident angles correlated closely with the simulation of impact on Armox 500 armoured plate, with a maximum deviation of 8.5%. Following validation, an optimized material model was implemented to further assess the armoured plate's ballistic resistance. The findings provide valuable insights into the resistance capabilities of the armoured plate, which can contribute to the defense sector.

Keywords*—High velocity impact, Johnson-Cook model, Ballistics, Armoured steel, Numerical simulation*

1. INTRODUCTION

Ballistics is the field of mechanics that deals with the motion, behavior, and effects of projectiles, especially ranged weapon munitions. Weapons that fire those munitions can be visualized as a single-stroke internal combustion engine where the projectile is the piston and the propellant is the air/fuel mixture. The impact of ballistics on any target can have several effects, ranging from penetration, perforation, plugging, fragmentation, etc [1].

Military and para-military sectors in Nepal are using various armored vehicles, bulletproof vests, and ballistic shields that supposedly provide the required protection from the ballistics in adverse situations. Such equipment makes use of armour steel plate, which protects vehicles, structures, and people from bullets, shrapnel, or explosive impacts. Due to its nature of use, the quality of such materials is a very sensitive factor. Despite its sensitivity, there is a limited study on the impact resistance of such armoured steel. This

has caused an increase in risk for the user as they can only validate those claims firsthand in adverse situations. If validation can be done about the protection level of those components based on the information provided about the material specified, it could be a huge asset for the people directly involved in handling the adverse situations. So, the research aims to evaluate the ballistic performance of armoured steel plate against high-speed projectiles through numerical simulation and experimentation.

2. LITERATURE REVIEW

The field of ballistics can be classified into four major disciplines: interior ballistics, intermediate ballistics, exterior ballistics, and terminal ballistics. Interior ballistics deals with the interaction of the gun, projectile, and propelling charge before the emergence of the projectile from the muzzle of the gun.

Intermediate ballistics deals with the initial motion of the projectile as it is exiting the muzzle of the tube. Exterior ballistics encompasses the period from when the projectile leaves the muzzle until impact with the target. Terminal ballistics covers aspects of events when the projectile reaches the target, such as penetration mechanics, blast overpressure, non-lethal effects, and effects on living tissue [1]. Terminal ballistics end effects are dependent on variables such as material properties, impact velocity, projectile shape, method of target support, and relative dimensions of projectile and target.

A. Effect of projectile velocity

Projectiles may impact a metallic target under a wide range of velocities. The nature of the target material is such that the different velocities must be handled using different techniques. At very low velocity (<0.5 km/s), the penetration is usually coupled to the overall structural dynamics of the target. The responses are on the order of 1 ms (high velocity impact dynamics). As the strike velocity increases (0.5-1.5 km/s), the response of the structure is dominated by the behavior of the material within a small zone (typically 2-3 projectile diameters) of the impact area. Typically, loading and reaction time are on the order of microseconds. Still further increase in impact velocity (2-3 km/s) results in localized pressure that exceeds by an order of magnitude the strength of the material [2].

B. Projectile configuration

Ball rounds are intended to attack lightly protected personnel and equipment. These consist of a lead alloy or mild steel core and a jacket. Ball rounds with a steel core have higher penetration and structural integrity compared with lead alloy cored ball rounds.

C. Failure of the target

During an impact event, the target response is a combination of global and local reactions. The relative contributions from these two reactions are generally determined

by a multitude of factors, such as strike velocity, projectile properties, target size, and boundary conditions. Typically, strike velocity is considered to be the most significant factor in determining the transition between locally dominated and globally dominated responses. It has been observed that the failure mechanisms at lower velocities are of global mode (referred to as transmitted stress wave), and it changes to local (shear or plug failure) at higher velocities [3].

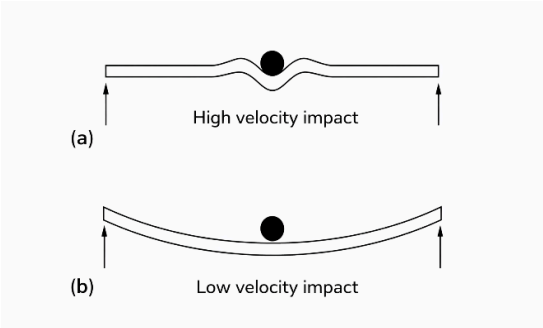

Figure 1: Representation of the impact response under (a) high velocity impact loading, (b) low velocity impact loading [4]

D. Numerical modeling

The finite element method (FEM) discretization is based upon a piecewise representation of the solution in terms of specified basis functions. The computational domain is divided into smaller domains (finite elements), and the solution in each element is constructed from the basic functions. Explicit dynamics is a numerical analysis method used to simulate how structures respond to fast, highly nonlinear, transient events—things like impacts, crashes, blasts, explosions, drop tests, and other short-duration, high-strain-rate problems.

The Johnson-Cook (JC) strength model is one of the most widely used material models in numerical simulations of high-strain-rate events like impact analysis, particularly for metals. It defines the hardening behavior of the material. The Johnson-Cook strength model [5] is expressed by equation (1).

$$Y = A(1 + \frac{B}{A}\varepsilon^{n})(1 + C\, ln\xi^{*})(1 + T^{m}) \quad (1)$$

where,

Y = Flow stress (the stress at which plastic deformation occurs)

A = Yield stress (initial yield strength at low strain rates and temperatures)

B = Hardening modulus (the material's resistance to plastic deformation at large strain)

n = Strain hardening exponent (controls the rate of increase of stress with strain)

C = Strain rate sensitivity parameter (increase of material strength with increase in strain rate)

ξ * = Non-dimensional reference strain rate

T = Normalized temperature (between 0 and 1, with 1 being the melting temperature)

m = Temperature sensitivity exponent (controls the effect of temperature on strength)

Five constants, A, B, C, n, and m, are characteristic of a given material. Information about these constants can be used to determine dynamic response during plastic deformation. The Johnson-Cook material model gives information about the stress-strain curve in the plastic range, so it is useful during computer simulation.

The Johnson-Cook failure model is a widely used numerical model that predicts ductile failure (fracture) in metals subjected to large strains, high strain rates, and high temperatures, which is the corresponding condition of impact analysis. The Johnson-Cook failure model indicates that the fracture strain generally depends on stress triaxiality ratio, temperature, and strain rate. The Johnson-Cook failure model [6] is given by equation (2):

$$\epsilon_f = [D_1 + D_2\, exp\,(D_3(\frac{\sigma_m}{\sigma_{eq}})][1 + D_4 ln(\dot{\epsilon}^*)][1 + D_5 T^*] \quad (2)$$

where, ϵ_f is the failure strain,

D_1 is the initial fracture strain,

D_2 is the exponential factor,

D_3 is the triaxiality factor,

D_4 is the strain rate parameter

D_5 is the temperature parameter.

σ_m is the mean stress and

σ_{eq} is the equivalent stress

The JC damage model suggests that damage builds up in the material element during plastic straining and accelerates immediately when the damage reaches a critical value. D is the damage variable, which varies between 0 (material not damaged) and 1 (fully failed material). Failure is assumed to occur when D reaches or exceeds the value of unity [7].

E. Research on high-speed impact

[8] studied normal and oblique impact on 20 mm thick AA6082-T4 Aluminium plates through both experimental testing and numerical simulations. Targets were impacted at angles 0^0, 15^0, 30^0, $45^{0,}$ and $60^{0,}$ and initial and residual velocities were measured by various laser-based optical devices. The penetration process was captured using high-speed video cameras. Material characterization tests were conducted to calibrate the modified Johnson-Cook constitutive relation and Latham failure criterion, while material data for the bullets were mainly taken from published literature. 3D nonlinear FE simulations were carried out, showing good overall agreement with experimental results.

[9] evaluated the ballistic limit of 500 HB armour steel subjected to 7.62 mm 54R B32 API hardened steel core ammunition. Lagrange and smoothed particle hydrodynamic (SPH) simulations were performed using a detailed 3D model of both the projectile and high-hardness armour target, and the result of Ls-Dyna simulations showed good agreement with experimental findings.

3. RESEARCH METHODOLOGY

During the research, the effect of the high velocity impact on the metal plates was simulated, and experiments were carried out to validate the simulated results. And finally, the numerical modeling and simulation were used to calculate the projectile resistance for the given armoured plate against projectiles with different configurations. The following steps are carried out during the research:

A. Material characterization of the target

Several experiments were conducted, and literatures were reviewed to outline the specifications, mechanical properties of the armoured steel target, and high-speed projectile. The target materials' hardness was tested using mico hardness tester. In this method of measuring hardness, a very small load is applied on a policed surface of material using a diamond indenter to form a small, well-defined indentation, as shown in Figure 2, and subsequently measuring the size of the indentation under a microscope. Calculated hardness values of the specimen are shown in Table 1.

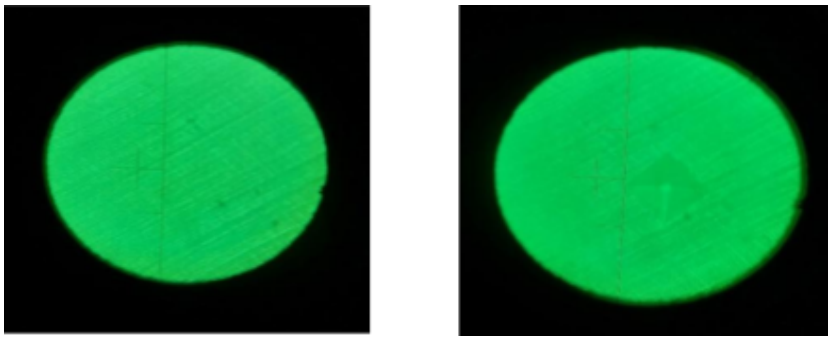

Figure 2: Hardness testing of armoured plate

Table 1: Vickers Hardness Number of Target Materials

S.N	Material	HV1	HV2	Avg HV
1	Armoured plate	506.6	512.9	509.75
2	MS plate	207.6	212	209.8

The hardness value of the armoured steel plate suggests that the armoured material can be of High Hardness Armour (HHA) steel, which has a hardness value in the range of 477-534 HV [10] . Other studies about Armox 500 armoured steel also suggest a hardness value of around 500 [9]. The mechanical properties of these armoured steels found in the literature are shown in Table 2.

Table 2: Mechanical properties of armoured plate

Property	Symbol	Value
Density	ρ	7850 kg/m^3
Youngs modulus	E	204.7 GPa
Poisson's ratio	ϑ	0.33
Source		[10]

The mechanical properties of both armoured steels are the same, regardless of harness grade, as this elastic property is determined by the fundamental iron lattice structure and shows minimal variation with alloying or heat treatment [11]. The Johnson-Cook material model parameters (A, B, n, C, m) and damage model parameters (D1, D2, D3, D4, D5) were extracted from the literature, as shown in Table 3. The dimension of the target used during the study was 300x300 mm and 6 mm thick.

Table 3: JC constitutive models constant

Description	Notation	Numerical Value (HHA Plate)	Numerical value (Armox 500)
Yield Stress constant	A	980 MPa	1470 Mpa
Strain hardening constant	B	2000 MPa	702 Mpa
Strain hardening exponent	n	0.83	0.199
Strain rate sensitivity effect	C	0.0026	0.00549
Thermal softening constant	m	1.4	0.811
Reference Strain rate	ξ *	0.0001s^{-1}	1
Melting Temperature	θ melt	1800	

Transition temperature	θ transition	293	
Fracture Strain constant	D1	0.05	0.068
	D2	0.8	5.382
	D3	-0.44	-2.551
	D4	-0.046	
	D5	0	
Source		[7]	[9]

B. Material characterization of the projectile

In this study 5.56 mm full metal jacket ball round is selected whose measurement is in accordance with STANAG 4172. The projectile is assembled from two components brass jacket and a lead alloy core. During impact testing, it is assumed that the brass jacket of the high-speed projectile is completely stripped off and the lead core actually hits the target. So, only the lead core has been modeled as the projectile for simulation [11]. Mechanical properties of the lead core obtained from the literature are shown in Table 4.

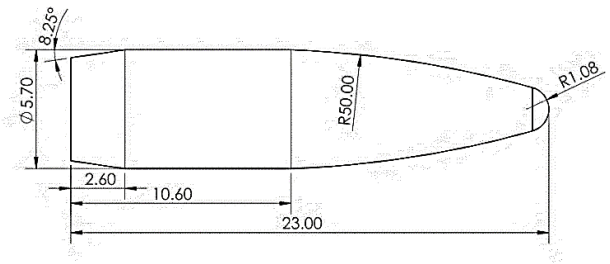

Figure 3: Dimension of 5.56 mm Nato round (mm)

Table 4: Mechanical properties of lead core

Property	Symbol	Value (Lead core)
Density	ρ	10940
Youngs modulus	E	$25.5x10^9$
Poisson's ratio	ϑ	0.4
Source		[12]

The Johnson Cook constant for lead and steel core projectile material was taken as shown in Table 5.

Table 5: JC constant for steel core [11]

Description	Notation	Numerical value (Lead core projectile)	Numerical value (Steel core AP projectile)
Yield Stress constant	A	$24x10^6$	$2700x10^6$
Strain hardening constant	B	$300x10^6$	$211x10^6$
Strain hardening exponent	n	1	0.065
Strain rate sensitivity effect	C	0.1	0.005
Thermal softening constant	m	1	1.17
Reference Strain rate	ξ *	$5x10^{-4}$	0.0001
Melting Temperature	θmelt	760	1800
Transition temperature	θtransition	293	293

C. Numerical simulation using FEA

The finite element method (FEM) implemented in an explicit solver was employed to simulate the high-velocity impact of the projectile and target. The explicit dynamics solver was used due to its ability to efficiently handle complex contact conditions, large material deformations, and transient dynamic phenomena relevant to ballistic impact. The following steps were carried out to develop a finite element model, including geometry, material definitions, contact interactions, mesh design, and analysis procedure.

a. Creating model parts

A three-dimensional model was created to represent the projectile and target corresponding to the ballistic test. The parts were created in 3D modeling software due to its simplicity and then imported into Abaqus for numerical simulation. The plate was fully fixed at its four edges to simulate a clamped boundary condition during the ballistic test, and an initial distance of 3 mm was set between the target and projectile to ensure a stable initial contact condition.

b. Defining materials and their properties

The accuracy of an impact simulation is critically dependent on the constitutive model used to represent material behavior under high strain. The armoured plate was modeled first as an HHA plate, then as an Armox 500 plate for simulation, and the simulation was conducted. Then the results of the simulation were compared with experimental data, and the material was finalized for further calculations based on the experimental results.

c. Contact interaction

A general contact algorithm was defined to manage all interactions within the model. A penalty-based contact formulation with a friction coefficient of 0.02 was specified for all surface-to-surface interactions [13].

d. Meshing strategy

A critical aspect of the model was the meshing strategy, which defines the accuracy. The armoured plate was partitioned to allow for a biased mesh, with a fine uniform mesh of size 0.5 mm equivalent to 1/12 of the diameter of the projectile in the central impact region up to a radial distance of 24 mm equivalent to 4 times the diameter of the projectile, and a gradually coarser mesh of size 5 mm towards the clamped boundaries. The projectile was meshed with a uniform mesh of element size 1.5 mm. A coarser element size is selected for the projectile as the study focuses on the ballistic performance of the target material rather than that of the projectile, and the smaller mesh size increases the computational complexity and thus the simulation time. All components were meshed with 8-node linear brick, reduced integration, and hourglass control (C3D8R) element, as these elements are computationally efficient and well-suited for large deformation and contact problems. The global mesh consists of 28805 elements on the target and 315 elements on the projectile material.

e. Assigning the initial input and boundary conditions

The initial velocity of the projectile was set to 918 m/s, corresponding to the terminal velocity of the M16 rifle. Based on STANAG 4172 specifications and experimental data [14], A velocity decay of 7.5% is observed over a 100 m distance, but for this calculation, it is assumed that the velocity during the impact will be equivalent to the terminal velocity. All four walls of the target were fixed, and the boundary conditions of the target were defined as such.

f. Step definition

A single dynamic, explicit step was created to simulate the impact event, and the step was set to 75 microseconds.

g. Interaction properties

Interaction properties define how surfaces interact when they contact each other. “Hard Contact” is selected, which assumes no pressure until they touch, and then infinite pressure. “Allow separation” is also selected as the projectile may rebound after impact.

h. Submitting and solving to get the desired result

Then, with the given input conditions and material properties, the state of the output is computed using an explicit dynamics solver.

4. RESULTS AND ANALYSIS

A. Simulation of projectile strike perpendicularly (90^0) to the surface of the target

The result of the projectile impact simulation at an impact angle of 90^0 is as shown in Figure 4. The projectile tip makes its first contact with the target within the first 5 µs, where the lead core deforms immediately due to its low yield strength. The projectile tip flattens against the armoured surface, and its material radiates outwards. The projectile is completely stopped within the first 50 µs, and then it bounces back. A permanent crater is formed in the impacting face of the armoured plate, and a minimal bulge is formed on the back face.

The simulation results using the HHA material model show a total energy variation of 5.7% during impact, while the projectile loses 89.79% of its initial kinetic energy, and the remaining energy is retained by scattered shrapnel. The maximum deformation of the surface was nearly equal to 2.06 mm, as in Figure 5.

Similarly, the simulation using Armox 500 material model had the total energy variation of 7.8% during impact, while the projectile loses 80.35% of its initial kinetic energy, and the remaining energy is retained by scattered sharpnels. The maximum deformation of the surface was nearly 1.96 mm, as in Figure 6. [15] Suggests that for explicit dynamics simulation of high-velocity impact, total energy variations within 5 – 10% are considered acceptable due to numerical dissipation from contact algorithm, hourglass control, and element erosion, and thus the variation of energy for this simulation is acceptable.

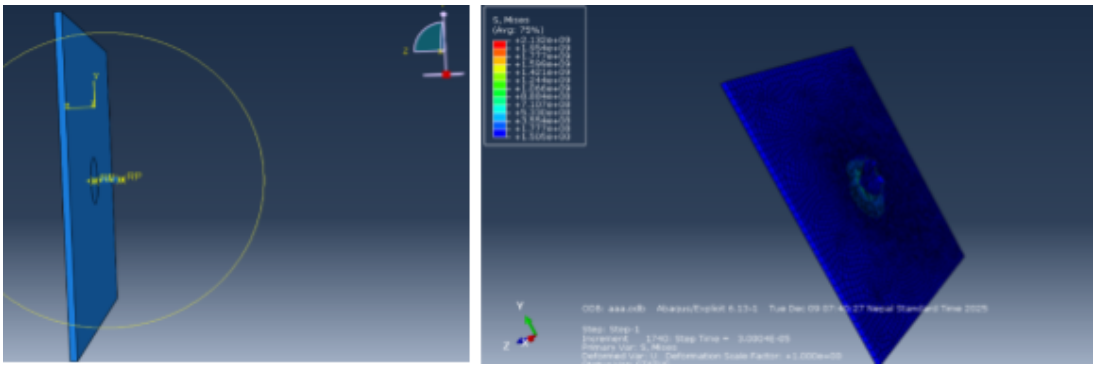

(a) (b)

Figure 4: Simulated result of 5.56 mm leaded core projectile at an angle of 60 0 (a) before impact (b) after impact

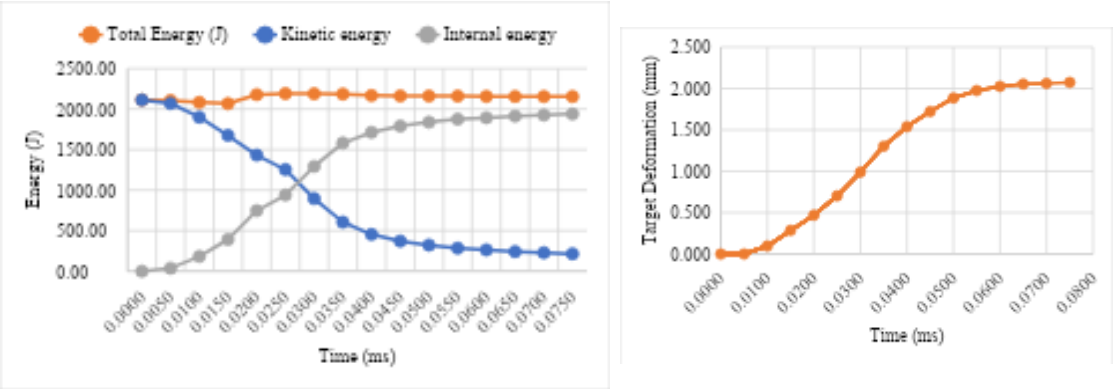

Figure 5: Graphical representation of 5.56 mm leaded core projectile impact perpendicularly on HHA armoured plate (a) Energy change with Time (b) Target Deformation with Time

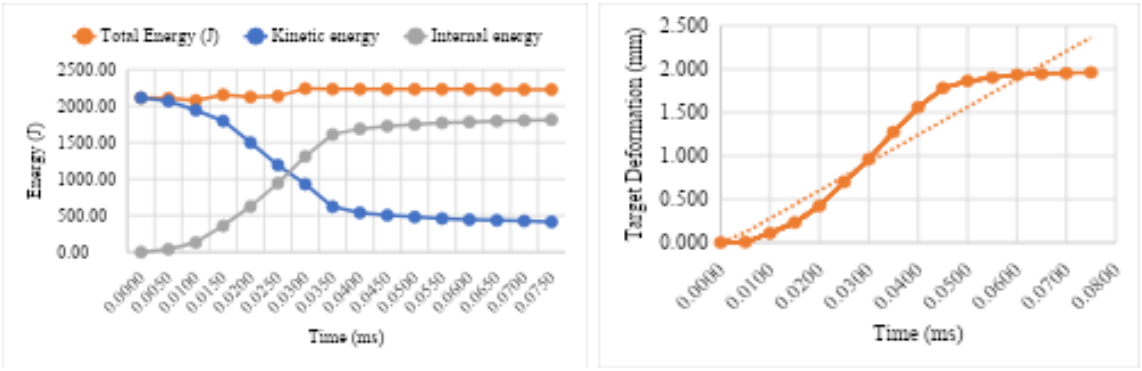

(a) (b)

Figure 6: Graphical representation of 5.56 mm leaded core projectile impact perpendicularly on Armox 500 armoured plate (a) Energy change with Time (b) Target Deformation with Time

B. Simulation of a projectile strike at an angle of 60^0 to the surface of the target

The result of the projectile impact simulation at an angle of 60^0 is shown in Figure 7-9. The projectile exhibits asymmetric mushrooming with severe deformation on the leading edge. The armoured surface develops a long, shallow deformation along the projectile sliding path before the projectile bounces off the target surface with an approximate overall velocity of 334 m/s for HHA, losing 86% of its initial kinetic energy, and 380 m/s for Armox 500 armoured plate, losing 82.6% of its initial kinetic energy. The residual energy is retained by the projectile that ricochets from the target.

The simulation results using the HHA material model showed a total energy variation of 6.97%, while the maximum deformation of the surface was nearly equal to 0.92 mm.

Similarly, the simulation using the Armox 500 material model, the total energy variation was of 4.11%, and the maximum deformation of the surface was nearly 0.81 mm.

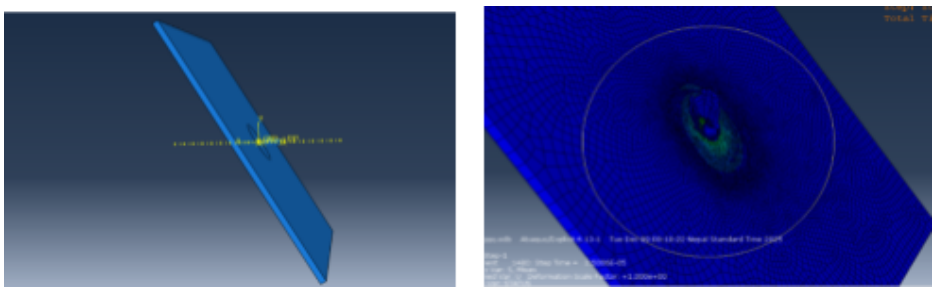

(a) (b)

Figure 7: Simulated result of 5.56 mm leaded core projectile at an angle of 60^{o} (a) before impact (b) after impact

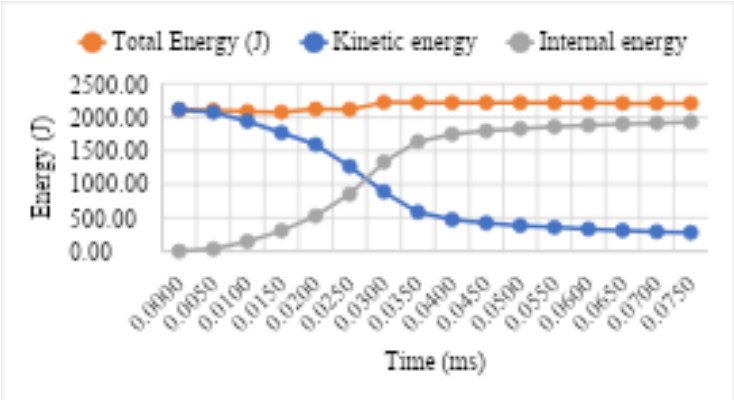

(a)

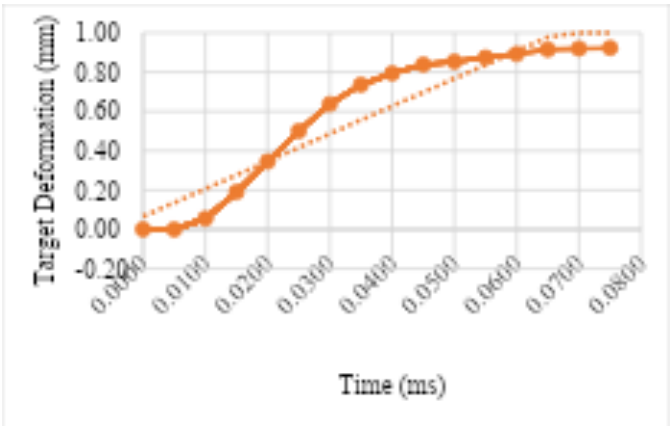

(b)

Figure 8: Graphical representation of 5.56 mm leaded core projectile impact at an angle of 60^{0} on HHA armoured plate (a) Energy change with Time (b) Target Deformation with Time

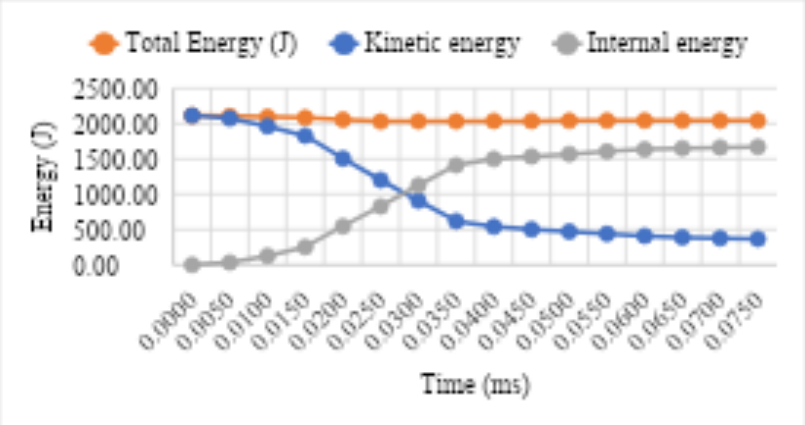

(a)

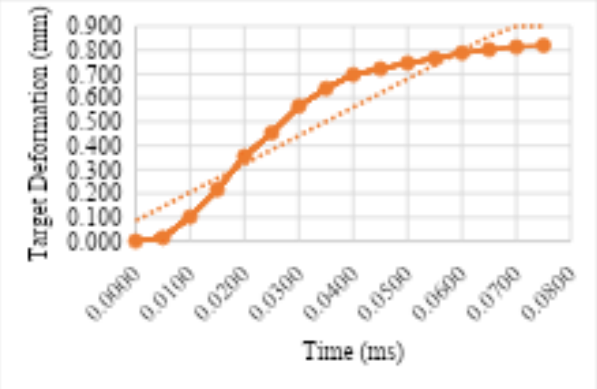

(b)

Figure 9: Graphical representation of 5.56 mm leaded core projectile impact at an angle of 60^0 on Armox 500 armoured plate (a) Energy change with Time (b) Target Deformation with Time

C. Simulation of a projectile strike at an angle of 30^0 to the surface of the target

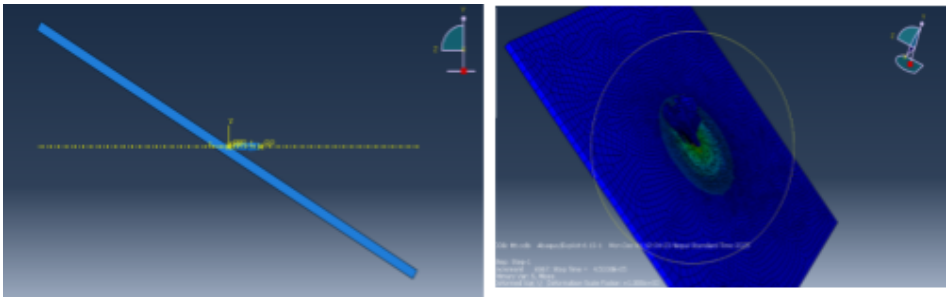

(a) (b)

Figure 10: Simulated result of 5.56 mm leaded core projectile impact at an angle of 30^0 (a) before impact, (b) after impact

The results shown in Figure 10 were similar to those during the impact of 60^0. The projectile exhibits severe asymmetric mushrooming with severe deformation on the leading edge. The armoured surface develops a long, shallow deformation along the projectile sliding path and then bounces off the target surface with residual velocity 795 m/s for HHA, losing only 24.5% of its initial kinetic energy, and 790 m/s for Armox 500 armoured plate, losing only 25.1% of its initial kinetic energy. The ricochet projectile is deformed but still carries high energy.

The simulation results using the HHA material model show a total energy variation of 5.95% while the maximum deformation of the surface was nearly equal to 0.48 mm, as in Figure 11. Similarly, the simulation using the Armox 500 material model, a total energy variation was of 4.98% and the maximum deformation of the surface was nearly 0.38 mm as shown in Fig 12.

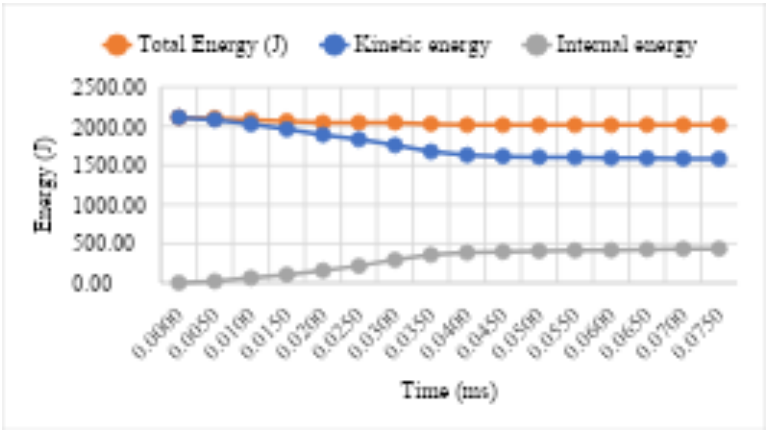

(a)

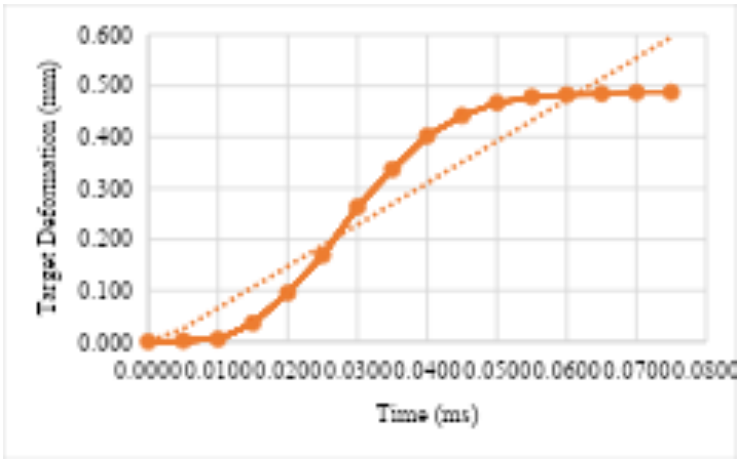

(b)

Figure 11: Graphical representation of 5.56 mm leaded core projectile impact at an angle of 30^0 on HHA armoured plate (a) Energy change with Time (b) Target Deformation with Time

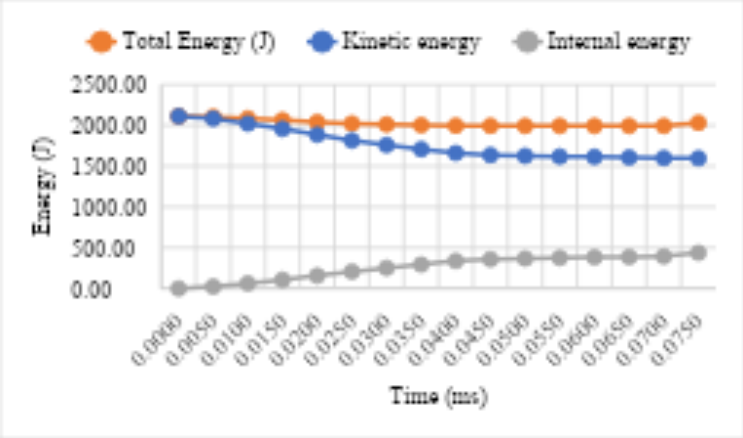

(a)

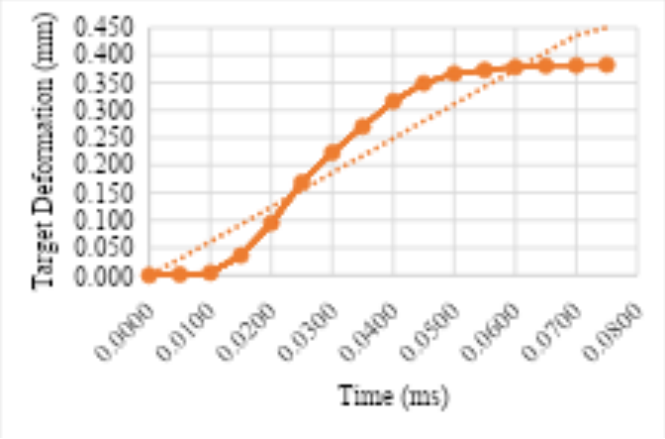

(b)

Figure 12: Graphical representation of 5.56 mm leaded core projectile impact at an angle of 30^0 on Armox 500 armoured plate (a) Energy change with Time (b) Target Deformation with Time

D. EXPERIMENTAL RESULTS

The experimentation was carried out inside a closed firing range where the projectile is fired from 50 m to the target. The target was mounted on a fixed stand inside a frame, and the angle of the frame can be adjusted by mounting the frame in a stand, as shown in Figure 13. The test material was experimented with while firing 5.56 mm leaded core high-speed projectiles at three incident angles obtained as 90^0, $64^{0,}$ and 36^0. The only deformation on the plate for each angle of incidence was measured and recorded to compare with the simulated result. As a limitation of the study, the experimental energy dissipation was not covered, whereas the simulated results have been compared.

The experimentation concluded that none of the projectiles could penetrate/perforate the armoured plate. The armoured plate is found to be resistant to the high-speed

projectile, and the impacted plates were shown in Figure 14. The deformation obtained during high-speed projectile impact can be listed in Table 6. The result suggests that the material modeling is suitable for the Aromox 500 armoured plate with a maximum deviation of 8.5% from the experimental result. The difference in the simulated result and experimental result may be due to the difference in the incident angle during simulation and experimentation.

Figure 13: Target stands at different incident angle configurations

(a) (b) (c)

Figure 14: Results of high-speed projectile impact on test plate (a) Perpendicular impact (b) Oblique impact at 60 degrees (c) Oblique impact at 30 degrees

Table 6: Experimental results of the deformation of the armoured plate at different incident angles of the projectile

S.N.	Angle of incidence	Deformation (Experiment)	Deformation (Simulated) (HHA)	Deviation (%)	Deformation (Simulated) (Armox 500)	Deviation (%)
1	90	1.93	2.06	6.7	1.96	1.55
2	64	0.77	0.92	19.5	0.81	5.19
3	36	0.35	0.48	37	0.38	8.5

E. Simulation of the impact of a 5.56 mm steel core projectile

The simulations were further carried out for a steel core projectile to observe its damage to the armoured plate. The simulated result shows that the armoured plate could successfully stop the projectile, while the projectile even bounced back, as in Figure 15. Almost all (>96%) kinetic energy is converted to plastic work and heat. The steel core of the projectile flattened and expanded radially while the armoured plate suffered deformation up to 2.969 mm, as in Figure 16. The back face shows visible bulging but remains intact.

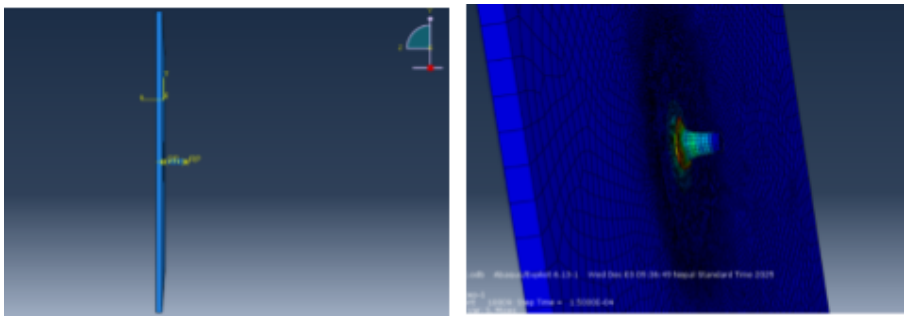

(a) (b)

Figure 15: Simulated result of 5.56 mm steel core projectile impact (a) before impact (b) after impact

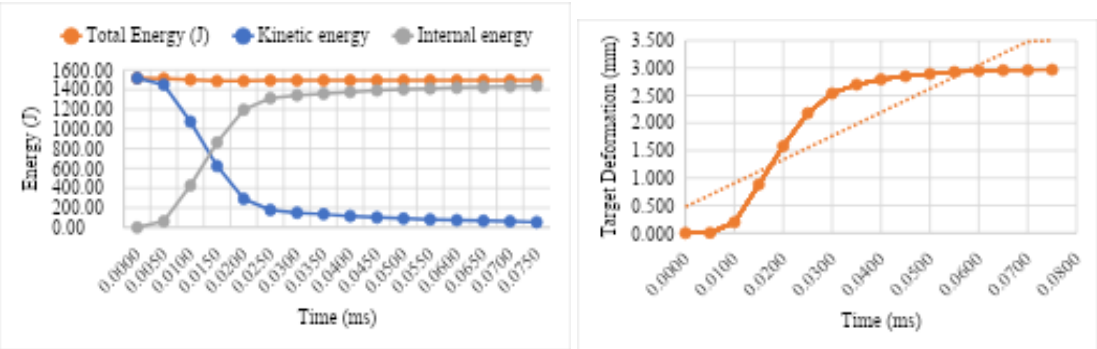

(a) (b)

Figure 16: Graphical representation of 5.56 mm steel core projectile impact perpendicularly (a) Energy with Time (b) Target Deformation with Time

F. Simulation of impact of 7.62 mm steel core projectile

The simulation is further carried out with a 7.62 mm steel core projectile. This simulation shows that the projectile is defeated but caused localized through-thickness failure, as in Figure 17. The impact velocity of the projectile is near the ballistic limit (V_{50}) as the projectile passes through the plate but remains embedded in it.

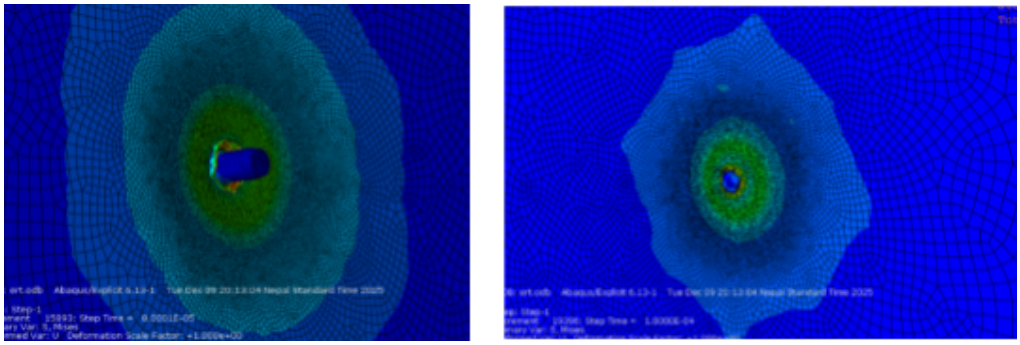

(a) (b)

Figure 17: Simulated result of 7.62 mm steel core projectile impact (a) Front face (b) Rear face

5. CONCLUSION

This research successfully developed and validated an experimental and finite element method using explicit dynamics with the JC model for evaluating the ballistic performance of armoured steel against high-speed projectiles. The hardness of the armoured plate was found to be 509.75 and this value suggests the material property to be of High Hardness Armour (HHA) steel or Armox 500. The experimental and simulated results correlated closely with the JC constants relating to Armox 500 steel plate. Further simulations suggest the armoured plate is capable of withstanding a 5.56 mm steel core projectile completely, while a 7.62 mm steel core projectile remained embedded in the plate. Those findings can be used as a performance prediction tool for assessing armoured steel performance against specific threats that can be helpful for defense sectors. Further study of the armoured plate should attempt to find the values of the JC constant by conducting experimentation on the target material. High-speed camera setup during impact experiment and equipment to observe steel deformation at small/micro scale assist in obtaining results that are more reliable and help in understanding the nature of failure of materials. Also, the study of material properties will be a stepping stone towards developing new materials with better ballistic resistance capabilities.

ACKNOWLEDGEMENT

This research has received no financial aid. The authors would like to acknowledge the Department of Automobile and Mechanical Engineering, Thapathali Campus, for providing support for this research work and would like to express sincere gratitude to the Nepali Army for providing equipment, materials, and space to conduct tests, without which the research would not have been possible.

REFERENCES

[1] S. S. J. Donald E. Carlucci, Ballistics theory and design of guns and ammunition, Taylor and Francis group, 2007.

[2] J. A. Zukas, "Impact Dynamics: Theory and experiment," US army armanent research and development command, Maryland, 1980.

[3] E. c. R. V. A. p. A shahkarami, "Material response to ballistic impact," The university of British Columbia, 2005.

[4] J. M. W. J. Cantwell, "Comparison of the low and high velocity impact response of CFRP," Composites, pp. 545-551, 1989.

[5] T. Pornpibunsompop, "Ballistic analysis of 14.5 AP bullet on Armour Material," in Asian conference on defence technology, Nonthnuri, Thailand, 2015.

[6] U. S. Burak Ozcan, "Determination of Johnson Cook Strength and Failure Parameters of EN-GJS-400 Spheroidal Graphite Cast Iron," Journal of Institute of science and technology, 2024.

[7] S. D. S. A. D. D. N. N. A. Banerjee, "Determination of Johnson cook material and failure model constants and numerical modeling of Charpy Impact test of armour steel," Materials science and engineering, pp. 200-209, 2015.

[8] L. O. S. D. M. L. Tore Borvik, "Normal and oblique impact of small arms bullet on AA6082-T4 aluminium protective plates," International journal of impact engineering, pp. 577-589, 2010.

[9] B. E. Namik Kilic, "Ballistic resistance of high hardness armoured steels against 7.62mm armoured piercing ammunition," Material and design, pp. 35-48, 2013.

[10] C. C. R. D. M. Teresa Fras, "Fracture of high-strength armour steel under impact loading," International journal of impact engineering, 2017.

[11] K. S. P. B. N. G. M.A. Iqbal, "The characterization and ballistic evaluation of mild steel," International Journal of Impact Engineering, pp. 98-113, 2016.

[12] Y. D. A. R. Yann Coget, "Characterization of the Mechanical Behavior of a Lead Alloy, from Quasi-Static to dynamic Loading for a wide range of temperatures," Materials, 20 May 2020.

[13] C. A. E. M. B. T. H. O. L. M. Borvik T, "Experimental and numerical study on the perforation of AA6005-T6 panels," International journal of impact engineering, pp. 35-64, 2005.

[14] J. J. K. Balter, "Experimental analysis of 5.56x45 mm NATO ball ammunition performance," Defence Technology, pp. 194-199, 2017.

[15] A. M. J. M. J. P. Latham, "Energy conservation in explicit finite element simulation of impact problems," International Journal for Numerical Methods in Engineering, pp. 1759-1767, 2000.